Available online at www.sciencedirect.com

ScienceDirect

Underground Space xxx (2018) xxx–xxx

www.elsevier.com/locate/undsp

Numerical modeling of high velocity impact applied to reinforced concrete panel

Chahmi Oucif [a,*], Luthfi Muhammad Mauludin [a,b]

[a] Institute of Structural Mechanics (ISM), Bauhaus-Universität Weimar, Marienstraße 15, D-99423 Weimar, Germany
[b] Teknik Sipil, Politeknik Negeri Bandung, Gegerkalong Hilir Ds.Ciwaruga, Bandung 40012, Indonesia

Received 14 February 2018; received in revised form 29 March 2018; accepted 23 April 2018

Abstract

A numerical simulation of a high-velocity impact of reinforced concrete structures is a complex problem for which robust numerical models are required to predict the behavior of the experimental tests. This paper presents the implementation of a numerical model to predict the impact behavior of a reinforced concrete panel penetrated by a rigid ogive-nosed steel projectile. The concrete panel has dimensions of 675 mm × 675 mm × 200 mm, and is meshed using 8-node hexahedron solid elements. The behavior of the concrete panel is modeled using a Johnson-Holmquist damage model incorporating both the damage and residual material strength. The steel projectile has a small mass and a length of 152 mm, and is modeled as a rigid element. Damage and pressure contours are applied, and the kinetic and internal energies of the concrete and projectile are evaluated. We also evaluate the velocity at different points of the steel projectile and the concrete panel under an impact velocity of 540 m/s.

Keywords: Johnson-Holmquist; High velocity impact; Reinforced concrete panel; Damage

1. Introduction

It is well known that concrete is much stronger in terms of compression than in tension. Because of its high compressive strength, and to enhance its tensile strength, tensile reinforcements are added to concrete elements subjected to tensile loading (Rabczuk & Belytschko, 2006; Rabczuk, Akkermann, & Eibl, 2005; Rabczuk, Zi, Bordas, & Nguyen-Xuan, 2008). A concrete material is subjected to static and dynamic loads. The static loads are permanent, whereas the dynamic loads vary over time. Among the dynamic loads, impact loads, which have catastrophic consequences on the structures, are included. An analysis of the impact behavior of reinforced concrete (RC) structures has been of significant interest in recent decades (Diyaroglu, Oterkus, Madenci, Rabczuk, & Rabczuk, 2016; Hu et al., 2017; Kalameh, Karamali, Anitescu, & Rabczuk, 2012; Levi-Hevroni, Kochavi, Kofman, Gruntman, & Sadot, 2018; Rabczuk & Eibl, 2006).

Numerous experimental investigations have been carried out on the impact behavior of reinforced concrete structures, through which the compressive strength of concrete has been highlighted to describe its influence on the impact resistance. Many results have shown that the impact resistance of RC concrete is improved when high strength concrete is used (Guo, Gao, Jing, & Shim, 2017; Luccioni et al., 2017). However, Hanchak, Forrestal, Young, and Ehrgott (1992) revealed an exception of this behavior through impact tests applied to concrete slabs penetrated by an ogive-nosed steel projectile using different amounts of unconfined compressive strength, namely, 48 and 140 MPa, and reinforced with 5.69 mm diameter bars.

* Corresponding author.
E-mail addresses: chahmi.oucif@uni-weimar.de (C. Oucif), luthfi.muhammad.mauludin@uni-weimar.de (L.M. Mauludin).

https://doi.org/10.1016/j.undsp.2018.04.007

The projectile perforation was undertaken with velocities of 300–100 m/s. The results of the experimental tests showed that an increase in the compressive strength has a minor influence on the impact resistance. Borvik, Langseth, Hopperstad, and Polanco-Loria (2002) carried out experimental ballistic penetration tests on fiber-reinforced high-performance concrete slabs penetrated by steel conical-nosed projectiles. The nominal compressive strengths of the concrete slabs were 75, 150, and 200 MPa. It was concluded that the ballistic limit velocity increases to a maximum of 20% even if the unconfined compressive strength of the concrete increases. Li, Wu, Hao, Wang, and Su (2016) studied the brittle behavior of concrete slabs, in which conventional and ultra-high performance concrete with different slab depths and spacing of the principal reinforcements were subjected to a contact explosion. The results showed that ultra-high performance concrete displays an improved resistance compared to conventional concrete. Othman and Marzouk (2016) conducted experimental tests to describe the effects of the steel reinforcement distribution on the dynamic behavior of reinforced concrete plates under impact loads. Their results showed that the impact energy is unaffected by variations in the ratio and distribution of a steel reinforcement when the same impact loads are applied. However, it was found that only the distribution of the steel reinforcement affects the crack pattern and failure mode. Rajput and Iqbal (2017) studied experimentally the ballistic performance of plain, reinforced, and pre-stressed concrete plates subjected to ogive-nosed steel projectiles with a diameter of 19 mm. The velocity applied during their experimental tests varied from 60 to 220 m/s. It was found that the reinforcement minimizes the scabbing and spalling of concrete.

Although experimental investigations are important, there is always an important need for the implementation of numerical models. Numerous numerical models have been implemented with regard to the impact behavior of reinforced concrete structures. Xu, Hao, and Li (2012) implemented a dynamic impact model on steel fiber-reinforced concrete (SFRC) samples in which the steel fibers, aggregates, and cement mortar content were taken into account in the description of the impact behavior of SFRC. It was shown that the ductility of SFRC increases when fibers are added to the concrete, and the stress and strain redistribution becomes clear in the presence of such fibers. It was also observed that an increase in the amount of fibers has a direct influence on the dynamic increase factor (DIF). Feng, Yao, Li, and Li (2017) conducted a numerical investigation on the impact behavior of a plain concrete slab penetrated by a steel projectile using the lattice discrete particles model (LDPM) when considering the interaction between constituents at the mesoscale. Navas, Yu, Li, and Ruiz (2018) developed a new mesh-free method to describe the behavior of brittle materials subjected to an explosion. Many other numerical investigations have demonstrated the importance of using a mesh-free method in the dynamic modeling of a fracture (Amiri, Anitescu, Arroyo, Bordas, & Rabczuk, 2014; Amiri, Millan, Shen, Rabczuk, & Arroyo, 2014; Bordas, Rabczuk, & Zi, 2008; Rabczuk & Belytschko, 2007; Rabczuk & Belytschko, 2010; Rabczuk, Areias, & Belytschko, 2010a, 2010b; Rabczuk, Bordas, & Askes, 2010a, 2010b; Zi, Rabczuk, & Wall, 2007), as well as multi-scale modeling (Budarapu, Gracie, Bordas, & Rabczuk, 2014; Budarapu, Gracie, Yang, Zhuang, & Rabczuk, 2014; Talebi, Silani, & Rabczuk, 2015; Talebi, Silani, Bordas, Kerfriden, & Rabczuk, 2014). In addition, recent insights have also been achieved in the area of fracture mechanics, in which different methods were used, such as a mesh refinement, phase field analysis, and element-wise based fracture models (Areias & Rabczuk, 2013; Areias & Rabczuk, 2017; Areias, Rabczuk, & Camanho, 2014; Areias, Rabczuk, & Dias-Da-Costa, 2013; Areias, Rabczuk, & Msekh, 2016; Areias, Reinoso, Camanho, César de Sá, & Rabczuk, 2017). Other impact models based on continuum damage mechanics have also been implemented (Areias, Msekh, & Rabczuk, 2016; Dunant, Bordas, Kerfriden, Scrivener, & Rabczuk, 2011; Silani, Talebi, Hamouda, & Rabczuk, 2016; Thai, Rabczuk, Bazilevs, & Meschke, 2016). Pereira, Weerheijm, and Sluys (2018) proposed a new damage model based on an effective rate-dependent framework to simulate the ballistic behavior of concrete structures. Ismail, Zairi, Nait-Abdelaziz, and Azari (2012) proposed a combined numerical and experimental approach to estimate the continuum damage stress limits of glass impacted by solid particles.

In the present paper, the impact behavior of a reinforced concrete panel penetrated by a rigid steel ogive-nosed projectile is numerically studied. The concrete material is modeled using the Johnson–Holmquist damage model (JH-2). An analytical rigid element with a reference point assigning its mass is used to simulate the steel projectile. A general contact surface with nodal erosion is adapted to simulate the contact between the projectile and concrete panel. The numerical commercial package Abaqus/Explicit is used in this paper. The variations in the velocity of the concrete panel and steel projectile at different points are described. We also evaluate the evolution of damage and pressure in the concrete panel, as well as the analysis of the kinetic energy of the projectile and the internal energy of the concrete panel under an impact velocity of 540 m/s.

2. Johnson–Holmquist damage model (JH-2)

Several constitutive models have been used for a description of the dynamic behavior of brittle materials under impact loads. In this paper, the Johnson-Holmquist damage model (JH-2) is used to analyze the impact behavior of a reinforced concrete panel penetrated by a steel ogive-nosed projectile. JH-2 is the second version of the Johnson–Holmquist (JH-1) ceramic model (Johnson & Holmquist, 1992), which is able to simulate the impact behavior of brittle materials, such as the dilatation, pressure-strength dependence, and strain-rate effects

Please cite this article in press as: Oucif, C., & Mauludin, L.M., Numerical modeling of high velocity impact applied to reinforced concrete panel, Underground Space (2018), https://doi.org/10.1016/j.undsp.2018.04.007

resulting from damage (Holmquist, Johnson, & Cook, 1993). According to the JH-2 model, the yield strength degrades with damage accumulation, whereas in the JH-1 model, the yield strength degrades when a critical amount of damage is reached. The strength is defined in terms of the equivalent stress as follows:

$$\sigma^* = \sigma_i^* - D(\sigma_i^* - \sigma_f^*) \tag{1}$$

where σ_i^* is the normalized intact equivalent stress, D is the damage variable, and σ_f^* is the normalized fractured equivalent stress. It should be noted that the intact and fully damaged materials are represented by the damage values $D = 0$ and $D = 1$, respectively. The equations of strength can also be defined in a general form by normalizing the terms in Eq. (1) to the equivalent stress at the Hugoniot elastic limit (HEL), which corresponds to a one-dimensional shock wave that exceeds the elastic limit as follows:

$$\sigma_{HEL} = \frac{3}{2}(HEL - P_{HEL}) \tag{2}$$

where P_{HEL} is the pressure at the HEL. After normalization, Eq. (1) can be rewritten as

$$\sigma^* = \frac{\sigma}{\sigma_{HEL}} \tag{3}$$

According to the JH-2 model, it is assumed that the equation of the strength in the case of undamaged and fully damaged material states can be expressed as a function of the pressure and strain rate, respectively, as follows:

$$\sigma_i^* = A(P^* + T^*)^N(1 + C\ln\varepsilon^*) \le \sigma_i^{max} \tag{4}$$

$$\sigma_f^* = B(P^*)^M(1 + C\ln\varepsilon^*) \le \sigma_f^{max} \tag{5}$$

where the material parameters are A, B, C, M, and N, and the strengths limits σ_i^{max} and σ_f^{max}. The normalized pressure is defined as

$$P^* = \frac{P}{P_{HEL}} \tag{6}$$

where P is the actual pressure. The normalized maximum tensile hydrostatic pressure is also written as

$$T^* = \frac{T}{T_{HEL}} \tag{7}$$

where T is the maximum tensile pressure supported by the material. The strain rate is given by $\dot{\varepsilon}^{pl} = \dot{\bar{\varepsilon}}^{pl}/\dot{\varepsilon}_0$, where $\dot{\bar{\varepsilon}}^{pl}$ is the equivalent plastic strain rate. The JH-2 model uses a similar damage accumulation of the Johnson-Cook model, and assumes that the damage increases along with the plastic strain as follows:

$$D = \sum \frac{\Delta\bar{\varepsilon}^{pl}}{\bar{\varepsilon}_f^{pl}(P)} \tag{8}$$

$$\bar{\varepsilon}^{pl} = D_1(P^* + T^*)^{D_2};\ \bar{\varepsilon}_{fmin}^{pl} \le \bar{\varepsilon}^{pl} \le \bar{\varepsilon}_{fmax}^{pl} \tag{9}$$

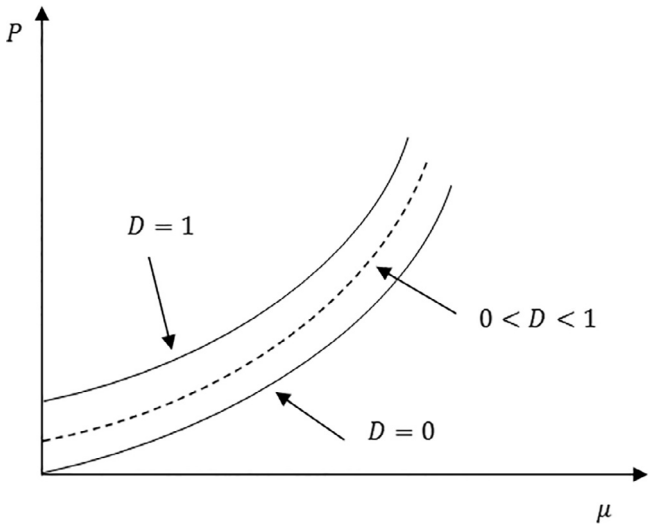

Fig. 1. Pressure–volumetric strain relationship of the JH-2 model.

It should be noted that $\Delta\bar{\varepsilon}^{pl}$ is the increment of the equivalent plastic strain, and $\bar{\varepsilon}_f^{pl}(P)$ is the equivalent plastic strain at failure. In addition, D_1 and D_2 are material constants. The parameters $\bar{\varepsilon}_{fmin}^{pl}$ and $\bar{\varepsilon}_{fmax}^{pl}$ are introduced for a limitation of the minimum and maximum values of the fracture strain. The pressure-volume relationship of a brittle material is defined as

$$\begin{cases} K_1\mu + K_2\mu^2 + K_3\mu^3 & if\ \mu \ge 0\ \text{(compression)} \\ K_1\mu & if\ \mu < 0\ \text{(tension)} \end{cases} \tag{10}$$

where K_1, K_2, and K_3 are material constants, and $\mu = \rho/\rho_0 - 1$, with ρ and ρ_0 indicating the current and reference densities, respectively. When a material fails, an additional pressure increment ΔP is included, which takes the following expression:

$$P = K_1\mu + K_2\mu^2 + K_3\mu^3 + \Delta P \tag{11}$$

The determination of the pressure increment is determined based on the energy considered. When the material is damaged, the deviatoric elastic energy ΔU decreases owing to the decrease in strength. Figure 1 shows the relationship of the pressure–volumetric strain according to the JH-2 model.

The decrease in elastic energy is converted into the potential energy through an increase in the pressure increment ΔP, such that

$$\Delta P_{t+\Delta t} = -K_1\mu_{t+\Delta t} + \sqrt{(K_1\mu_{t+\Delta t} + \Delta P_t)^2 + 2\beta K_1\Delta U} \tag{12}$$

where β is the fraction of the elastic energy increase converted into potential energy ($0 \le \beta \le 1$).

3. Constitutive material model

Among the different dimensions of RC panels available, Wu, Fang, Peng, Gong, and Kong (2015) experimentally investigated the impact behavior of a reinforced concrete

Please cite this article in press as: Oucif, C., & Mauludin, L.M., Numerical modeling of high velocity impact applied to reinforced concrete panel, Underground Space (2018), https://doi.org/10.1016/j.undsp.2018.04.007

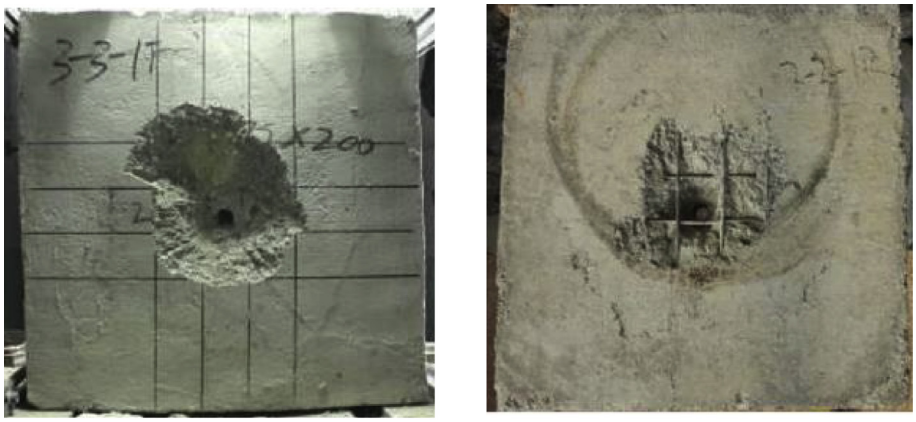

(a) (b)

Fig. 2. Damage to (a) font and (b) rear surfaces of RC panel (Wu et al., 2015).

panel with dimensions of 675 mm × 675 mm × 200 mm penetrated with a steel ogive-nosed projectile at velocities ranging from 540 to 745 m/s. Figure 2 illustrates the front and rear surfaces of the damaged target (675 mm × 675 mm × 200 mm) after application of the impact test conducted by Wu et al. (2015). The concrete panel is internally reinforced with three orthogonal layers of steel with a diameter of 6 mm, and the concrete cover is about 15 mm in depth. The geometry of the steel ogive-nosed projectile is 152 mm in length and 25.30 mm in diameter, with a caliber-radius-head (CRH) ratio of 3.0. Figure 3 shows the geometry configurations of the reinforced concrete panel and the steel ogive-nosed projectile. The reinforced concrete panel is modeled using the JH-2 model with the commercial package Abaqus/Explicit. The parameters of the JH-2 model are taken from (1993) (see Table 1). The projectile is modeled as an analytical rigid element with a mass assigned at a reference point with an initial velocity of 540 m/s. General contact between the projectile and surface of the concrete panel is considered. In the experimental impact tests of the reinforced concrete panel (Wu et al., 2015), it was considered that the projectile should be consistently impacted between the steel reinforcement, which neglects the effects of the steel reinforcement on the impact resistance. It was demonstrated by Huang, Wu, Jin, and Zhang (2005) that a steel reinforcement does not have an effect on the resistance of a concrete target under an impact load because the diameter of the projectile is much smaller than the grid size of the steel reinforcement. Therefore, in the present work, the panel is considered to be plain concrete to simplify the numerical simulation. With the aim to save computational costs, only the half of the concrete

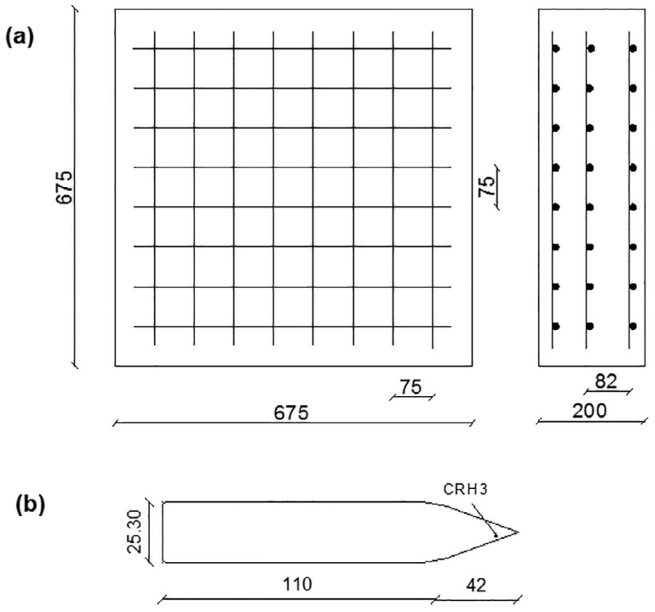

Fig. 3. Geometry of (a) reinforced concrete panel and (b) steel projectile (dimensions in mm).

Table 1
Material parameters of the concrete material (Holmquist and Johnson. 1993).

ρ (kg/m^3)	G (GPa)	A	B	n	C	
2440	14.86	0.79	1.6	0	0.007	
m	$\dot{\varepsilon}_0$	S_{max}	T (GPa)	$\bar{\varepsilon}^{pl}_{fmin}$	$\bar{\varepsilon}^{pl}_{fmax}$	P_{HEL} (MPa)
0.61	1	7	0.00354	0.001	1	48
D_1	D_2	K_1 (GPa)	K_2 (GPa)	K_3 (GPa)	HEL (MPa)	
0.04	1	85	−171	208	80	

Please cite this article in press as: Oucif, C., & Mauludin, L.M., Numerical modeling of high velocity impact applied to reinforced concrete panel, Underground Space (2018), https://doi.org/10.1016/j.undsp.2018.04.007

panel and projectile is considered, as shown in Fig. 4. A three-dimensional eight-node reduced integration (C3D8R) element was adopted with a 5 mm × 5 mm × 5 mm mesh at the impact location, and 20 mm × 20 mm × 20 mm mesh in the outer region.

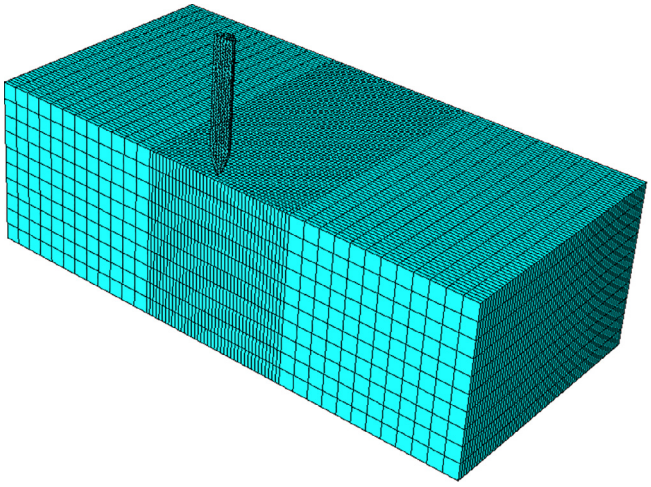

Fig. 4. Finite element discretization of one-half of the concrete panel and steel projectile.

4. Results and discussions

4.1. Damage and pressure contours

Figures 5 and 6 show the distribution of pressure and damage in the concrete panel, respectively, during the penetration of the steel projectile at a velocity of 540 m/s. The damage variable takes a value of 0.0 and 1.0 when the material is undamaged and totally damaged, respectively. The pressure is positive and ranges from 0 to 1.35×10^7 N/m^2, which corresponds to the amount of compression. It can be seen from Fig. 6 that the damage starts to initiate at the impact region with an expansion of the fracture around this region. From the plot of the pressure contour at time $t = 0.000\ 4$ s, it can be seen that the compressive wave passed through the thickness of the concrete panel, and a tensile wave developed in the free region at the middle of the concrete panel. This tensile wave resulted in an increase in the damage variable at the bottom edge of the

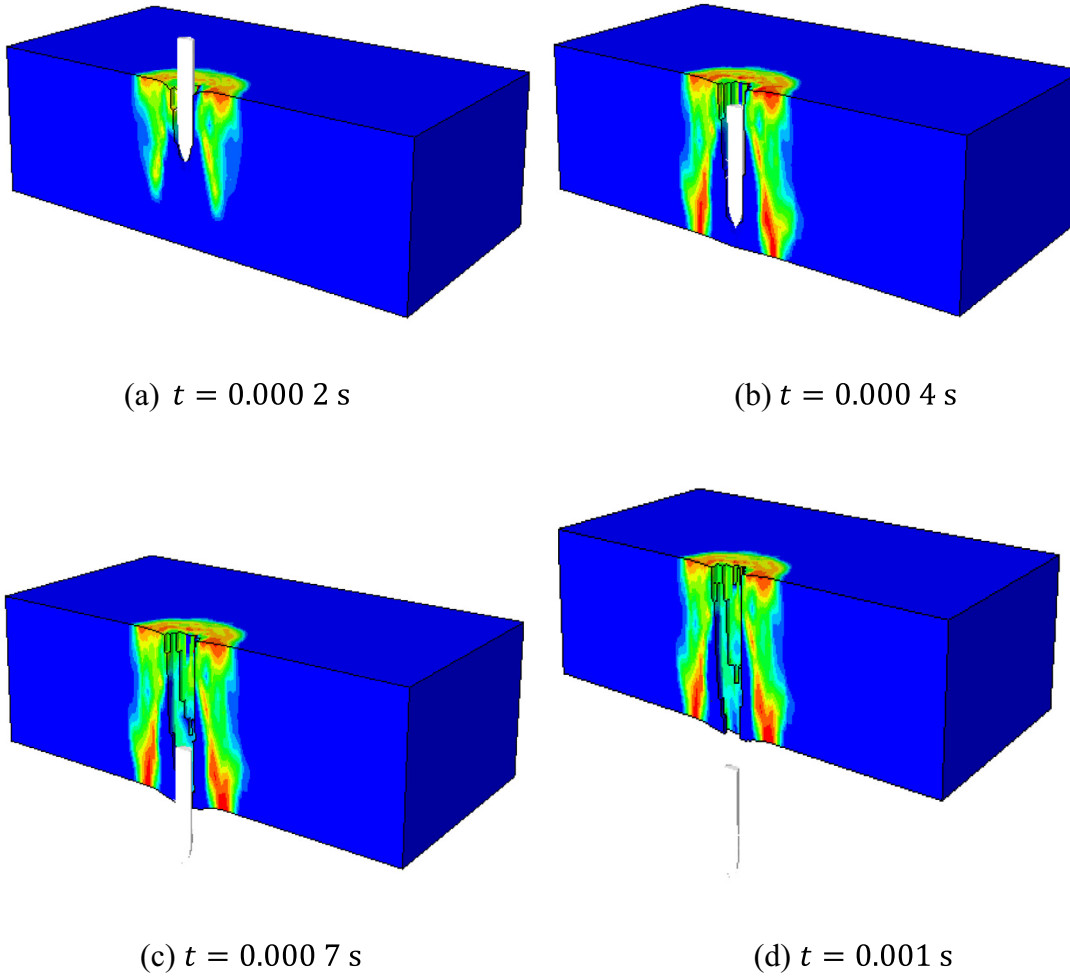

Fig. 5. Distribution of pressure in the concrete panel.

Please cite this article in press as: Oucif, C., & Mauludin, L.M., Numerical modeling of high velocity impact applied to reinforced concrete panel, Underground Space (2018), https://doi.org/10.1016/j.undsp.2018.04.007

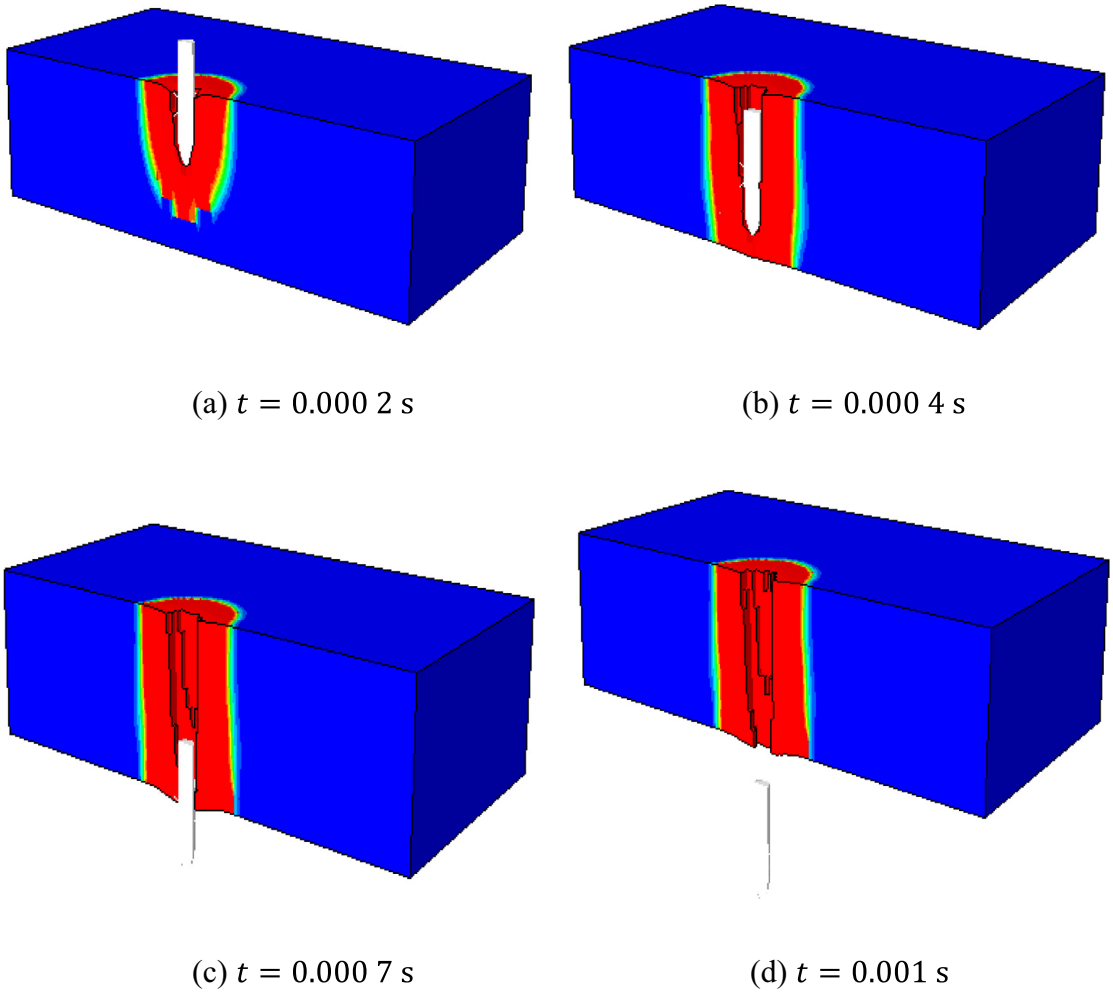

(a) $t = 0.000\ 2$ s (b) $t = 0.000\ 4$ s

(c) $t = 0.000\ 7$ s (d) $t = 0.001$ s

Fig. 6. Distribution of damage contour in the concrete.

concrete panel. It can also be seen that the concrete panel is completely perforated at time $t = 0.001$ s owing to its large thickness, which can consequently reduce the velocity of the projectile and absorb the impact energy.

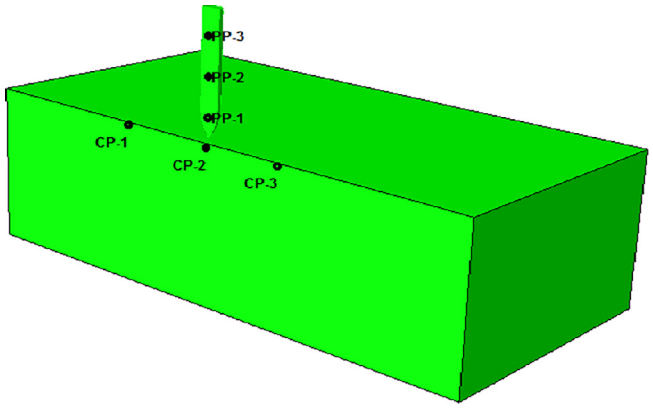

Fig. 7. Reference points in the concrete panel and rigid projectile.

4.2. Kinetic and internal energies and velocity analysis

In this section, the kinetic energy of the projectile and the internal energy of the concrete panel are analyzed under an impact velocity of 540 m/s. We also evaluate the velocity of the projectile and concrete panel at different points under the same impact velocity of 540 m/s (see Fig. 7). Figure 8 shows the kinetic energy of the projectile and the internal energy of the concrete panel under the 540 m/s of impact velocity. It can be clearly seen from Fig. 8 that the kinetic energy of the projectile gradually decreases when the projectile starts to penetrate into the concrete panel. On the other hand, it is also observed that the internal energy of the concrete panel increases linearly until a time of 500 μs when the concrete panel is completely penetrated by the projectile, and the final kinetic energies of the projectile and concrete panel are 29.10 kJ and 24.30 kJ, respectively.

Figures 9 and 10 show the evolution of the velocity of the projectile (PP-1, PP-2, and PP-3) and concrete panel (CP-1, CP-2, and CP-3), respectively, at different points

Please cite this article in press as: Oucif, C., & Mauludin, L.M., Numerical modeling of high velocity impact applied to reinforced concrete panel, Underground Space (2018), https://doi.org/10.1016/j.undsp.2018.04.007

under an impact velocity of 540 m/s. From Fig. 9, it can be clearly seen that the initial velocity of the projectile is 540 m/s, which decreases after the penetration of the concrete panel, and the velocity evolution at the three points of the projectile are similar because the projectile is assumed to be a rigid body. In addition, it can be clearly observed that at $t = 0.000\ 4$ s the velocity of the projectile starts to become stable, which is due to the full penetration of the projectile into the concrete panel, which matches the results illustrated in Fig. 5. From Fig. 10, it can be clearly seen

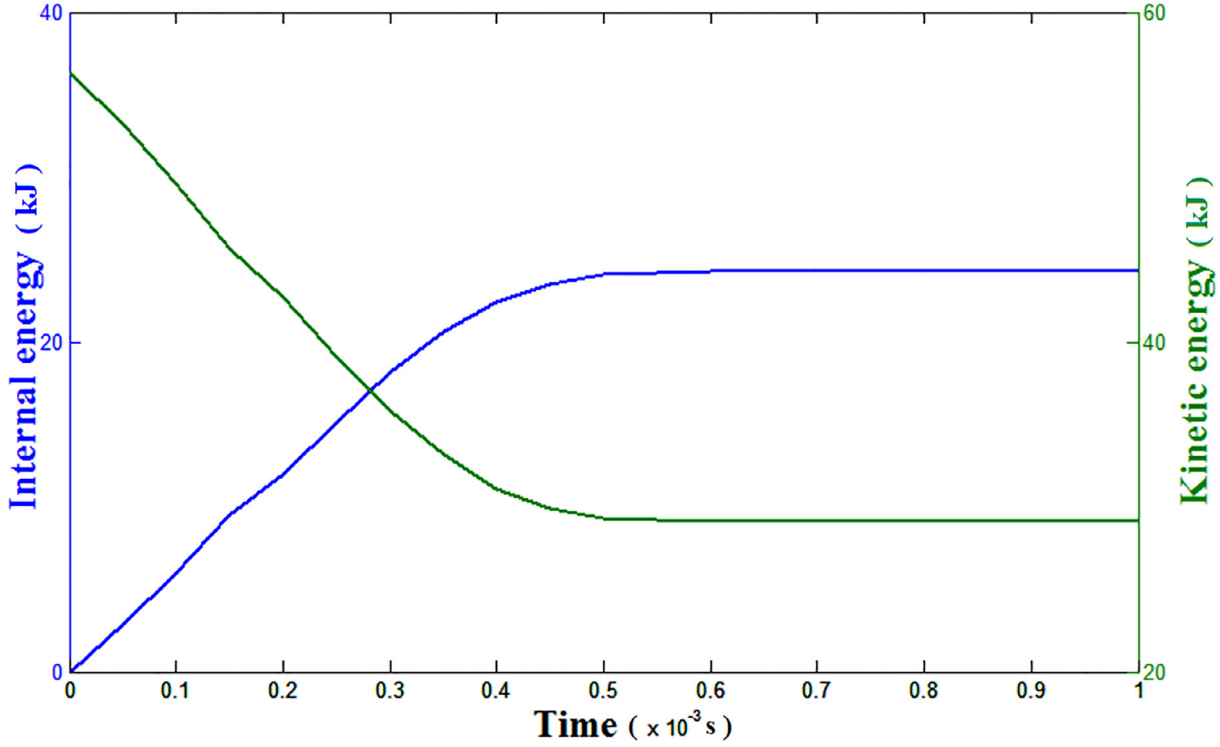

Fig. 8. Kinetic energy of projectile and internal energy of concrete under an impact velocity of 540 m/s.

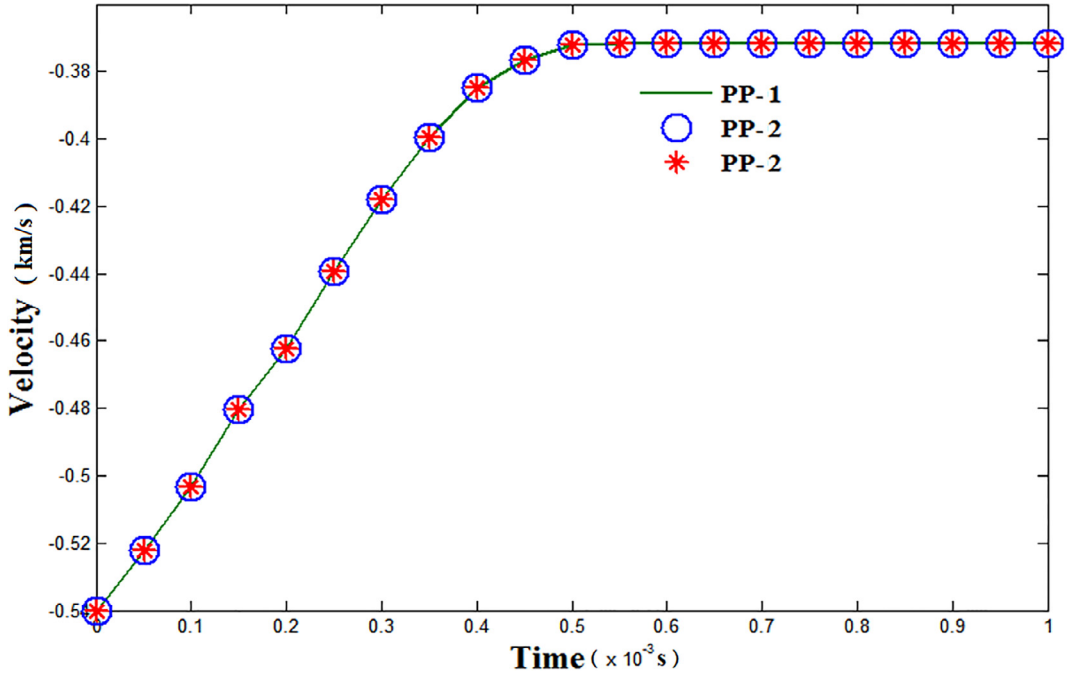

Fig. 9. Evolution of the velocity of the three points in the projectile.

Please cite this article in press as: Oucif, C., & Mauludin, L.M., Numerical modeling of high velocity impact applied to reinforced concrete panel, Underground Space (2018), https://doi.org/10.1016/j.undsp.2018.04.007

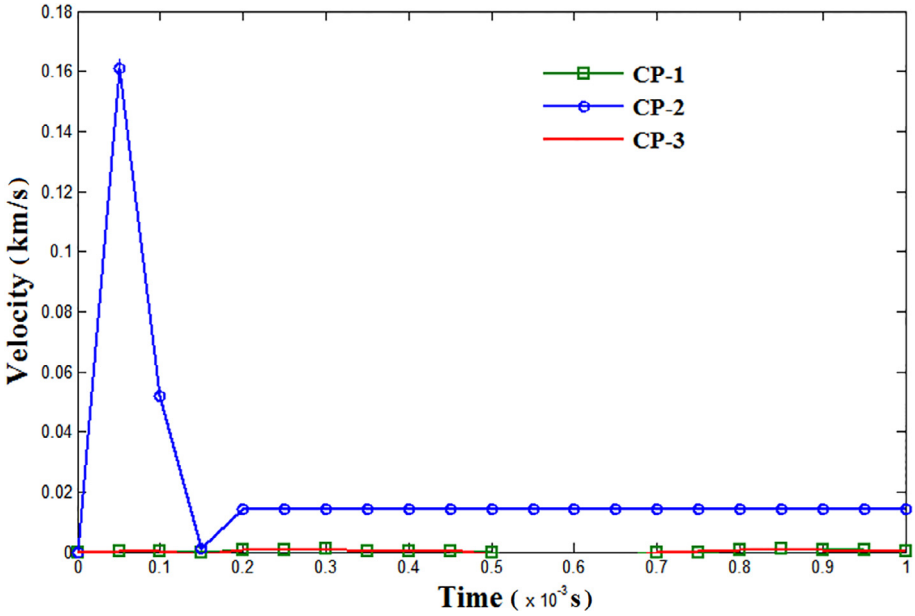

Fig. 10. Evolution of the velocity of the three points in the concrete panel.

that the residual velocity at the point CP-2 is higher than the residual velocities at the points CP-1 and CP-3. This can be explained by the fact that point CP-2 is directly subjected to the impact load, and is separated from the other two points, which are not subjected to a high impact load.

5. Conclusion

A numerical simulation of the penetration of a high-velocity impact through a reinforced concrete panel was simulated in this work. Because of the neglected effects of the steel reinforcement on the impact resistance of reinforced concrete structures, the simulated target was considered as plain concrete. The concrete material was modeled using the Johnson–Holmquist damage model (JH-2), and the steel ogive-nosed projectile used was simulated as a rigid body with a mass of 0.386 kg assigned at a reference point. The variations in velocity at different points of the projectile and concrete panel, as well as the damage and pressure, were evaluated. Analyses of the internal energy of the concrete panel and the kinetic energy of the steel projectile were also conducted. The kinetic energy of the projectile was shown to decrease, and once the projectile penetrates into the concrete panel, the panel tended to absorb the energy of the projectile, and thus enhancing stability of the projectile. It was found that the results of the kinetic and internal energies fit the results of the damage and pressure in terms of the penetration time of the projectile into the concrete panel as well as the impact behavior. It was shown that the Johnson–Holmquist damage model (JH-2) can be utilized to describe the impact behavior of a plain concrete panel. Future work may focus on an analysis of the influence of the spatial and time discretizations, and the uncertain input parameters on the results of the impact modeling.

Conflict of interest

The authors declared no conflict of interest.

Acknowledgements

The first author would like to acknowledge Deutscher Akademischer Austauschdienst (DAAD) for their financial support of this work. The second author would like to acknowledge RISTEK-DIKTI (Directorate General of Resources for Science, Technology and Higher Education, Ministry of Research, Technology, and Higher Education of Indonesia) under funding agreement No. 153.39/E4.4/2014.

References

Amiri, F., Anitescu, C., Arroyo, M., Bordas, S. P. A., & Rabczuk, T. (2014). XLME interpolants, a seamless bridge between XFEM and enriched meshless methods. *Computational Mechanics, 53*(1), 45–57.

Amiri, F., Millan, D., Shen, Y. X., Rabczuk, T., & Arroyo, M. (2014). Phase field modeling of fracture in linear thin shells. *Theoretical and Applied Fracture Mechanics, 69*, 102–109.

Areias, P., Msekh, M. A., & Rabczuk, T. (2016). Damage and fracture algorithm using the screened Poisson equation and local remeshing. *Engineering Fracture Mechanics, 158*, 116–143.

Areias, P., & Rabczuk, T. (2013). Finite strain fracture of plates and shells with configurational forces and edge rotations. *International Journal for Numerical Methods in Engineering, 94*(12), 1099–1122.

Areias, P., & Rabczuk, T. (2017). Steiner-point free edge cutting of tetrahedral meshes with applications in fracture. *Finite Elements in Analysis & Design, 132*, 27–41.

Areias, P., Rabczuk, T., & Camanho, P. P. (2014). Finite strain fracture of 2d problems with injected anisotropic softening elements. *Theoretical and Applied Fracture Mechanics, 72*, 50–63.

Areias, P., Rabczuk, T., & Dias-Da-Costa, D. (2013). Element-wise fracture algorithm based on rotation of edges. *Engineering Fracture Mechanics, 110*(3), 113–137.

Areias, P., Rabczuk, T., & Msekh, M. A. (2016). Phase-field analysis of finite-strain plates and shells including element subdivision. *Computer Methods in Applied Mechanics & Engineering, 312*, 322–350.

Areias, P., Reinoso, J., Camanho, P. P., César de Sá, J., & Rabczuk, T. (2017). Effective 2D and 3D crack propagation with local mesh refinement and the screened Poisson equation. *Engineering Fracture Mechanics*.

Bordas, S., Rabczuk, T., & Zi, G. (2008). Three-dimensional crack initiation, propagation, branching and junction in non-linear materials by an extended meshfree method without asymptotic enrichment. *Engineering Fracture Mechanics, 75*(5), 943–960.

Borvik, T., Langseth, M., Hopperstad, O. S., & Polanco-Loria, M. (2002). Ballistic perforation resistance of high performance concrete slabs with different unconfined compressive strengths. *WIT Transactions on The Built Environment*, 59.

Budarapu, P. R., Gracie, R., Bordas, S. P. A., & Rabczuk, T. (2014). An adaptive multiscale method for quasi-static crack growth. *Computational Mechanics, 53*(6), 1129–1148.

Budarapu, P. R., Gracie, R., Yang, S. W., Zhuang, X., & Rabczuk, T. (2014). Efficient coarse graining in multiscale modeling of fracture. *Theoretical & Applied Fracture Mechanics, 69*(2), 126–143.

Diyaroglu, C., Oterkus, E., Madenci, E., Rabczuk, T., & Rabczuk, T. (2016). Peridynamic modeling of composite laminates under explosive loading. *Composite Structures, 144*, 14–23.

Dunant, C. F., Bordas, S. P. A., Kerfriden, P., Scrivener, K. L., & Rabczuk, T. (2011). An Algorithm to compute damage from load in composites. *Frontiers of Architecture & Civil Engineering in China, 5*(2), 180–193.

Feng, J., Yao, W. J., Li, W. X., & Li, W. (2017). Lattice discrete particle modelling of plain concrete perforation responses. *International Journal of Impact Engineering, 109*, 39–51.

Guo, Y. B., Gao, G. F., Jing, L., & Shim, V. P. W. (2017). Response of high-strength concrete to dynamic compressive loading. *International Journal of Impact Engineering, 108*, 114–135.

Hanchak, S. J., Forrestal, M. J., Young, E. R., & Ehrgott, J. Q. (1992). Perforation of concrete slabs with 48 MPa (7 ksi) and 140 MPa (20 ksi) unconfined compressive strengths. *International Journal of Impact Engineering, 12*(12), 1–7.

Holmquist, T. J., Johnson, G. R., & Cook, W. H. (1993). A computational constitutive model for concrete subjected to large strains, high strain rates and high pressures. Ballistics international symposium 2 warhead mechanisms terminal ballistics. *Quebec, 2*, 591–600.

Hu, F., Wu, H., Fang, Q., Liu, J. C., Liang, B., & Kong, X. Z. (2017). Impact performance of explosively formed projectile (EFP) into concrete targets. *International Journal of Impact Engineering, 109*, 150–166.

Huang, F., Wu, H., Jin, Q., & Zhang, Q. (2005). A numerical simulation on the perforation of reinforced concrete targets. *International Journal of Impact Engineering, 32*(1), 173–187.

Ismail, J., Zairi, F., Nait-AbdelaCziz, M., & Azari, Z. (2012). How cracks affect the contact characteristics during impact of solid particles on glass surfaces: A computational study using anisotropic continuum damage mechanics. *International Journal of Impact Engineering, 40*(2), 10–15.

Johnson, G. R., & Holmquist, T. J. (1992). A computational constitutive model for brittle materials subjected to large strains, high strain rates and high pressures. *Shock Wave and HighStrain Rate Phenomena in Materials*, 1075–1081.

Kalameh, H. A., Karamali, A., Anitescu, C., & Rabczuk, T. (2012). High velocity impact of metal sphere on thin metallic plate using smooth particle hydrodynamics (SPH) method. *Frontiers of Structural & Civil Engineering, 6*(2), 101–110.

Levi-Hevroni, D., Kochavi, E., Kofman, B., Gruntman, S., & Sadot, O. (2018). Experimental and numerical investigation on the dynamic increase factor of tensile strength in concrete. *International Journal of Impact Engineering, 114*, 93–104.

Li, J., Wu, C., Hao, H., Wang, Z., & Su, Y. (2016). Experimental investigation of ultra-high performance concrete slabs under contact explosions. *International Journal of Impact Engineering, 93*, 62–75.

Luccioni, B., Isla, F., Codina, R., Zerbino, R., Giaccio, G., & Torrijos, M. C. (2017). Effect of steel fibers on static and blast response of high strength concrete. *International Journal of Impact Engineering, 107*, 23–37.

Navas, P., Yu, R. C., Li, B., & Ruiz, G. (2018). Modeling the dynamic fracture in concrete: An eigensoftening meshfree approach. *International Journal of Impact Engineering, 113*, 9–20.

Othman, H., & Marzouk, H. (2016). An experimental investigation on the effect of steel reinforcement on impact response of reinforced concrete plates. *International Journal of Impact Engineering, 88*, 12–21.

Pereira, L. F., Weerheijm, J., & Sluys, L. J. (2018). Simulation of compaction and crushing of concrete in ballistic impact with a new damage model. *International Journal of Impact Engineering, 111*, 208–221.

Rabczuk, T., Akkermann, J., & Eibl, J. (2005). A numerical model for reinforced concrete structures. *International Journal of Solids & Structures, 42*(5), 1327–1354.

Rabczuk, T., Areias, P. M. A., & Belytschko, T. (2010b). A simplified mesh-free method for shear bands with cohesive surfaces. *International Journal for Numerical Methods in Engineering, 69*(5), 993–1021.

Rabczuk, T., Areias, P. M. A., & Belytschko, T. (2010a). A meshfree thin shell method for non-linear dynamic fracture. *International Journal for Numerical Methods in Engineering, 72*(5), 524–548.

Rabczuk, T., & Belytschko, T. (2006). Application of particle methods to static fracture of reinforced concrete structures. *International Journal of Fracture, 137*(1–4), 19–49.

Rabczuk, T., & Belytschko, T. (2007). A three-dimensional large deformation meshfree method for arbitrary evolving cracks. *Computer Methods in Applied Mechanics & Engineering, 196*(29), 2777–2799.

Rabczuk, T., & Belytschko, T. (2010). Adaptivity for structured meshfree particle methods in 2D and 3D. *International Journal for Numerical Methods in Engineering, 63*(11), 1559–1582.

Rabczuk, T., Bordas, S., & Askes, H. (2010b). Meshfree methods for dynamic fracture. *Computational Technology Reviews, 1*, 157–185.

Rabczuk, T., & Eibl, J. (2006). Modelling dynamic failure of concrete with meshfree methods. *International Journal of Impact Engineering, 32*(11), 1878–1897.

Rabczuk, T., Bordas, S., & Askes, H. (2010c). Meshfree discretization methods for solid mechanics. Encyclopedia of aerospace engineering.

Rabczuk, T., Zi, G., Bordas, S., & Nguyen-Xuan, H. (2008). A geometrically non-linear three-dimensional cohesive crack method for reinforced concrete structures. *Engineering Fracture Mechanics, 75*(16), 4740–4758.

Rajput, A., & Iqbal, M. A. (2017). Ballistic performance of plain, reinforced and prestressed concrete slabs under normal impact by an ogival-nosed projectile. *International Journal of Impact Engineering, 110*, 57–71.

Silani, M., Talebi, H., Hamouda, A. M., & Rabczuk, T. (2016). Nonlocal damage modelling in clay/epoxy nanocomposites using a multiscale approach. *Journal of Computational Science, 15*, 18–23.

Talebi, H., Silani, M., Bordas, S. P. A., Kerfriden, P., & Rabczuk, T. (2014). A computational library for multiscale modeling of material failure. *Computational Mechanics, 53*(5), 1047–1071.

Talebi, H., Silani, M., & Rabczuk, T. (2015). Concurrent multiscale modeling of three dimensional crack and dislocation propagation. *Advances in Engineering Software, 80*, 82–92.

Thai, T. Q., Rabczuk, T., Bazilevs, Y., & Meschke, G. (2016). A higher-order stress-based gradient-enhanced damage model based on isogeometric analysis. *Computer Methods in Applied Mechanics and Engineering, 304*, 584–604.

Wu, H., Fang, Q., Peng, Y., Gong, Z. M., & Kong, X. Z. (2015). Hard projectile perforation on the monolithic and segmented RC panels with a rear steel liner. *International Journal of Impact Engineering, 76*, 232–250.

Xu, Z., Hao, H., & Li, H. N. (2012). Mesoscale modelling of fibre reinforced concrete material under compressive impact loading. *Construction and Building Materials, 26*(1), 274–288.

Zi, G., Rabczuk, T., & Wall, W. (2007). Extended meshfree methods without branch enrichment for cohesive cracks. *Computational Mechanics, 40*(2), 367–382.

Please cite this article in press as: Oucif, C., & Mauludin, L.M., Numerical modeling of high velocity impact applied to reinforced concrete panel, Underground Space (2018), https://doi.org/10.1016/j.undsp.2018.04.007